Molecular Dynamics Simulation of the Internal Mobilities in Molten $(Dy_{1/3},K)Cl$

Masahiko Matsumiya and Ryuzo Takagi[a]

Matsumiya Computational Chemistry Institute, 6-14 higashi-numa, machiya-aza, chiaki-cho, ichinomiya-shi, Aichi 491-0813 Japan
[a] Research Laboratory for Nuclear Reactors, Tokyo Institute of Technology, O-okayama, Meguro-ku, Tokyo 152-8550 Japan

Reprint requests to Prof. M. M.; Fax: 81 586-76-6473; E-mail: molten@d9.dion.ne.jp

Z. Naturforsch. **56a,** 273–278 (2001); received January 22, 2001

Molecular dynamics simulations have been performed on molten $(Dy_{1/3},K)Cl$ at 1093 K in order to compare the calculated self-exchange velocity (SEV), self-diffusion coefficient (D) and electrical conductivity with the corresponding experimental results. It was found that SEV, v, and D of potassium decrease with increasing concentration of dysprosium, as expected from the internal mobility, b. The decrease of b_K, v_K, and D_K are ascribed to the tranquilization effect by Dy^{3+} which strongly interacts with Cl^-. On the contrary, b_{Dy}, v_{Dy}, and D_{Dy} increase with increasing concentration of Dy^{3+}. This may be attributed to the stronger association of Dy^{3+} with Cl^- due to the enhanced charge asymmetry of the two cations neighboring to the Cl^-. In addition, the sequence of the calculated SEV's, D's and electrical conductivities for the various compositions were consistent with those of the referred experimental results.

Key words: Electrical Conductivity; Internal Cation Mobility; Molten $DyCl_3$-KCl; Molecular Dynamics Simulation; Self-exchange Velocity; Self-diffusion Coefficient.

1. Introduction

In [1] we have developed a pyrochemical process for electronegative elements, introducing countercurrent electromigration [2] into the electrowinning systems [3–7] following the Argonne National Laboratory's suggestion [8]. In addition, we have previously performed an estimation of the enrichment degree for the molten alkali ternary chlorides (Li, Na, Cs) Cl [9], (Li, K, Cs) Cl [10], (Na, K, Cs) Cl [11] and the fluoride (Li, Na, Cs)F [9] by MD simulation. We also previously demonstrated that the multivalent cations such as La^{3+} [12], Nd^{3+} [13], and Dy^{3+} [14] were easily separated by electromigration because the difference in the mobilities of alkali cations and rare earth cations is large. Thus, this countercurrent electromigration induced us to study the internal cation mobility in molten $DyCl_3$-KCl mixtures, since dysprosium is one of the main fission products among the electronegative elements. Pure KCl and $DyCl_3$ was also simulated for comparison with $(Dy_{1/3},K)Cl$. Few studies on self-exchange velocities in multivalent-monovalent mixtures seem to exist so far.

2. The Molecular Dynamics Simulation

The MD simulation of molten KCl, $DyCl_3$ and $(Dy_{1/3},K)Cl$ was done with more than 1000 Cl^- ions placed in a basic cube with periodic boundaries, the side length L of which was determined from the molar volume calculated from those of the pure melts on the assumption of additivity. Pair potentials of the Born-Mayer-Huggins type were employed

$$\Phi_{ij} = \frac{z_i\, z_j\, e^2}{4\pi\, \varepsilon_0\, r} + A_{ij}\, b \exp\left[(\sigma_i + \sigma_j - r)/\varrho\right] - \frac{c_{ij}}{r^6} - \frac{d_{ij}}{r^8}\,, \qquad (1)$$

$$A_{ij}\left(1 + \frac{z_i}{n_i} + \frac{z_j}{n_j}\right), \qquad (2)$$

where z_i and z_j are the formal charges of the ions i and j, r is the distance between two particles, b and ϱ are repulsion energy, and c_{ij} and d_{ij} dispersion energy parameters, e is the elementary charge, σ_i and σ_j are ionic radii, ε_0 is the permittivity of vacuum and A the Pauling factor. The first term in (1) represents the Coulomb interaction, the second the Born-Huggins exponential repulsion with parameters provided by Tosi and Fumi [15], while the third and fourth terms represent the di-

0932-0784 / 01 / 0300-0273 $ 06.00 © Verlag der Zeitschrift für Naturforschung, Tübingen · www.znaturforsch.com

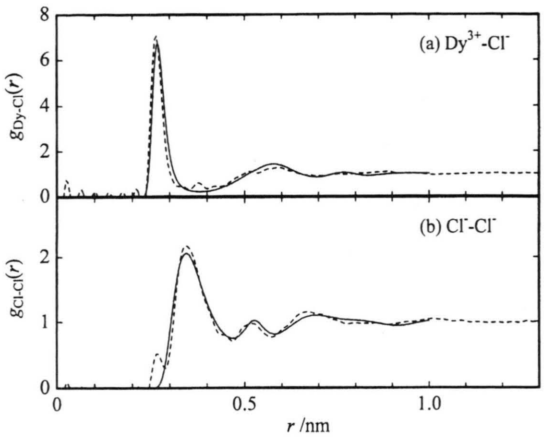

Fig. 1. Pair correlation functions of molten $DyCl_3$. (a) $g_{Dy\text{-}Cl}(r)$ calculated: solid line, experimental: broken line. (b) $g_{Cl\text{-}Cl}(r)$ calculated: solid line, experimental: broken line.

Table 1. The parameters employed in the calculation for molten $(Dy_{1/3},K)Cl$.

Dy:K	Ion Pair	ϱ/nm	$c_{ij}/10^{-79}$ $J \cdot m^6$	$d_{ij}/10^{-99}$ $J \cdot m^8$
(0:100)	K-K	0.337	24.3	24.0
	K-Cl		48.0	73.0
	Cl-Cl		124.5	250.0
(24:76)	Dy-Cl	0.3353	67.419	0.0
	K-Cl		48.256	0.0
	Cl-Cl		122.742	0.0
(42:53)	Dy-Cl	0.3341	67.104	0.0
	K-Cl		48.122	0.0
	Cl-Cl		121.389	0.0
(53:47)	Dy-Cl	0.3333	66.904	0.0
	K-Cl		48.034	0.0
	Cl-Cl		120.545	0.0
(67:33)	Dy-Cl	0.3323	66.642	0.0
	K-Cl		47.916	0.0
	Cl-Cl		119.453	0.0
(76:24)	Dy-Cl	0.3317	66.468	0.0
	K-Cl		47.836	0.0
	Cl-Cl		118.740	0.0
(84:16)	Dy-Cl	0.3311	66.311	0.0
	K-Cl		47.763	0.0
	Cl-Cl		118.100	0.0
(91:9)	Dy-Cl	0.3306	66.171	0.0
	K-Cl		47.696	0.0
	Cl-Cl		117.535	0.0
(95:5)	Dy-Cl	0.3304	66.090	0.0
	K-Cl		47.658	0.0
	Cl-Cl		117.210	0.0
(100:0)	Dy-Cl	0.3300	46.570	0.0
	K-Cl		65.988	0.0
	Cl-Cl		116.802	0.0

$\sigma_{Dy} = 0.1530$ nm, $\sigma_K = 0.1463$ nm, $\sigma_{Cl} = 0.1585$ nm

pole-dipole and dipole-quadrupole dispersion energies with parmeters given by Mayer [16]. The dipole-quadrupole term for $DyCl_3$ and $(Dy_{1/3},K)Cl$ were excluded, as was the case for $(Dy_{1/3},Na)Cl$ [17]. The potential parameters, such as the ionic radius and softness parameter, were predicted from reproducing the experimental pair correlation functions [18] for $DyCl_3$ at 1100 K as shown in Fig. 1 and from the data of $(Dy_{1/3},Na)Cl$. The corresponding parameters for the mixture were determined by the combination rule given by Larsen et al. [19]. More detailed data of the adopted values of A, b, ϱ, r, c, and d are listed in Table 1. The Ewald method [20] was employed for the calculation of the Coulomb forces; the cutoff distance in real space was $L/2$, and the reciprocal lattice vectors $|\boldsymbol{n}^2|$ were counted up to 27. The convergence parameter a was $5.6/L$ and the time step 5 fs. At the beginning, MD runs were conducted with the constant temperature method of Woodcock [21]. After attainment of constant temperature by running several thousand steps, these were converted to constant energy runs. From the runs during more than 10^4 time steps, using Verlet's Algorithm after attainment of equilibrium, the structure and the other properties were obtained.

3. Results and Discussion

The pair correlation function $g(r)$ and the running coordination numbers $n(r)$ for increasing concentration of Dy are shown in Fig. 2 a–d. Some characteristic properties of $g(r)$ and $n(r)$ numbers are summarized in Table 2. Comparison of the pair correlation functions of

Table 2. Characteristic values of the $g_{ij}(r)$'s for cation-anion and anion-anion pairs. R_1 and R_2 are the distances where $g_{ij}(r)$ crosses unity for the first and second time, respectively, R_M and R_m are the distances at the first maximum and minimum, respectively. $n_{eq}(R_2-R_m)$ is the partial equivalent coordination number within R_2-R_m of a cation, which is equal to the coordination number of Cl^- around the cation.

System (Dy:K)	Ion Pair	R_1/nm	R_M/nm	$g(R_M)$	R_2/nm	R_m/nm	$n_{eq}(R_2-R_m)$
(24:76)	Dy-Cl	0.239	0.264	11.86	0.313	0.390	6.20–6.63
	K-Cl	0.316	0.348	1.71	0.429	0.528	5.74–8.36
(42:58)	Dy-Cl	0.238	0.265	10.01	0.313	0.383	6.23–6.74
	K-Cl	0.307	0.343	2.30	0.451	0.514	6.49–8.60
(67:33)	Dy-Cl	0.241	0.267	8.24	0.313	0.376	6.09–6.70
	K-Cl	0.300	0.337	2.77	0.442	0.495	6.56–8.85
(84:16)	Dy-Cl	0.241	0.267	7.43	0.311	0.381	6.03–6.82
	K-Cl	0.296	0.335	3.36	0.428	0.493	6.17–9.44
(100:0)	Dy-Cl	0.242	0.267	6.71	0.313	0.395	5.94–7.01

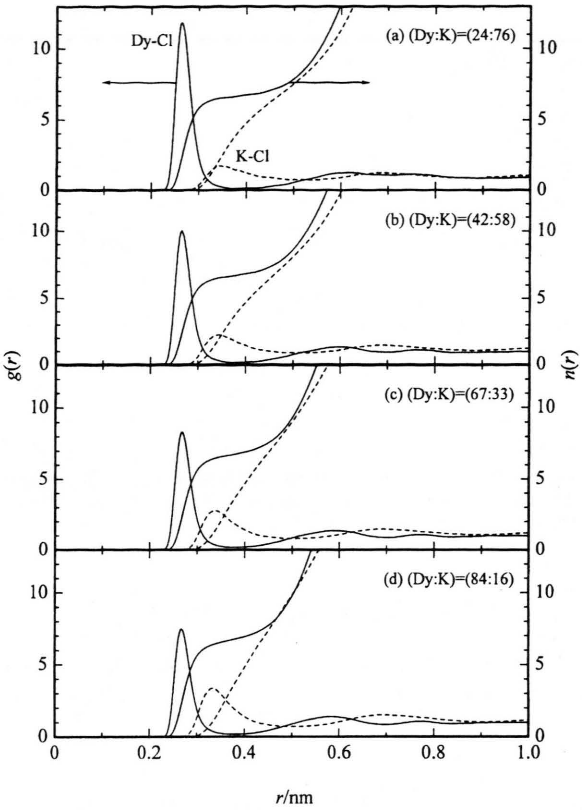

Fig. 2. Calculated pair correlation functions $g(r)$ and running coordination numbers $n(r)$ of molten $(Dy_{1/3}, K)Cl$ for four compositions. $g_{Dy\text{-}Cl}(r)$ and $n_{Dy\text{-}Cl}(r)$: solid lines, $g_{K\text{-}Cl}(r)$ and $n_{K\text{-}Cl}(r)$: broken lines.

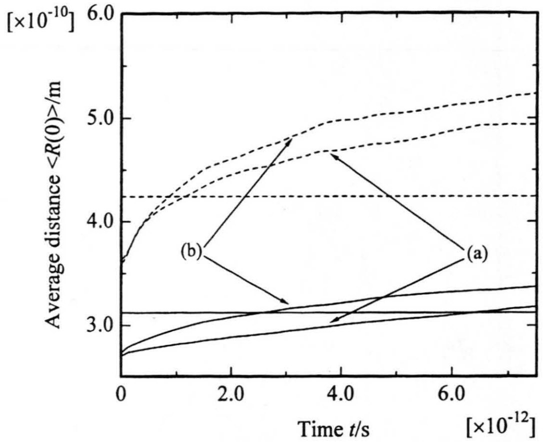

Fig. 3. Evolution in molten $(Dy_{1/3}, K)Cl$ of the average distance of marked cation from Cl^-. Solid lines: K^+; broken lines Dy^{3+}, (a) $x_{Dy} = 0.24$, (b) $x_{Dy} = 0.84$.

pure $DyCl_3$ and KCl with those of the binary mixtures shows that the position R_M of the first peak of $g_{Dy\text{-}Cl}$ remains much the same. As for the peak heights, $g_{Dy\text{-}Cl}$ is larger in the binary mixtures than in pure $DyCl_3$. On the contrary, $g_{K\text{-}Cl}$ is larger in the binary mixtures than in the pure KCl.

The separating motion of cation-anion pairs can be expressed in terms of the self-exchange velocity (SEV). The evolution of the average distance of marked Dy^{3+} and K^+ ions from a Cl^- ion for two compositions is shown in Figure 3. The SEV, v, which is correlated with internal mobility [22], is defined by

$$v = \frac{(R_2 - \langle R(0) \rangle)}{\tau}, \qquad (3)$$

where R_2 is the distance where the pair correlation function between cation and anion reaches unity after the first peak, and $\langle R(0) \rangle$ is the average distance of cations located within R_2 from a reference anion at $t = 0$. $t = \tau$ is the average time in which the average distance of such particles becomes R_2. Thus, the SEV is the velocity of the separating motion of two neighboring unlike ions and can be calculated with good accuracy from quite short MD simulation steps, since each anion has several neighboring cations. For the present system the SEV was calculated from 150 origins for the molten binary mixtures. The solid and broken lines in Fig. 3 show R_2 for Dy and K, respectively. The obtained SEVs for Dy and K are tabulated in Table 3, which shows that the SEV of Dy is smaller than that of K at all compositions. We have already demonstrated the strong correlation between internal mobilities and SEVs for some alkali chlorides [11, 22]. The relationship between the internal cation mobility [14], b, and the SEV, v, in our case is shown in Figure 4. The b values of K^+ and Dy^{3+} are calculated using the ε values of [14] and data available on the electrical conductivities κ [23] and the equivalent volumes V_e [23] of the mixtures

$$b_K = (\kappa V_e / F)\,(1 + \varepsilon x_{Dy}), \qquad (4a)$$

$$b_{Dy} = (\kappa V_e / F)\,(1 - \varepsilon x_K), \qquad (4a)$$

where x is the equivalent fraction. The decrease of b_{Dy} and SEV_{Dy} with decreasing concentration of Dy^{3+} is mainly caused by the charge-asymmetry rather than by the increase in the equivalent volume: Owing to the charge asymmetry of the coordinating cations about the Cl^- ions and consequently associates such as $[DyCl_6]^{3-}$ will have a longer life time. Raman spectroscopic stud-

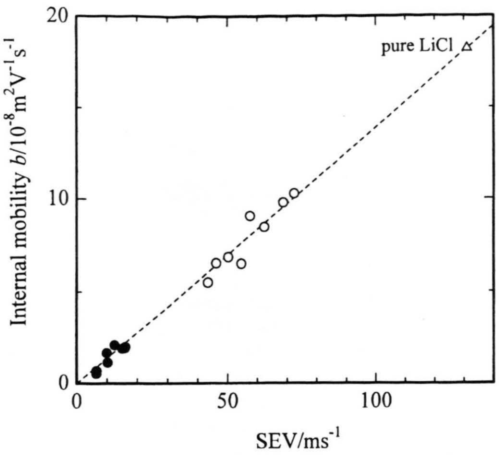

Fig. 4. Relationship between the internal cation mobility and self-exchange velocity in molten $(\mathrm{Dy}_{1/3},\mathrm{K})\mathrm{Cl}$, Dy^{3+}: black circles, K^+: white circles. Li^+ in pure LiCl [22]: white triangle.

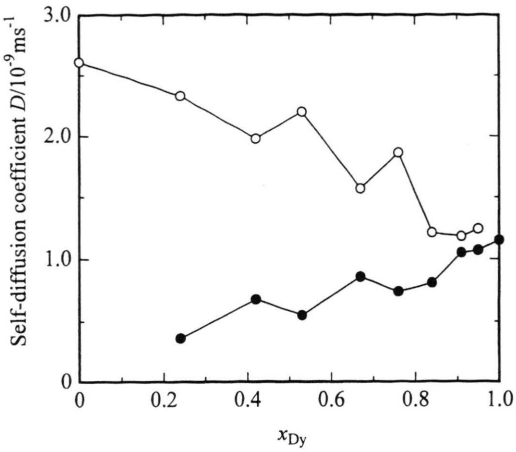

Fig. 5. Relationship between the self-diffusion coefficient and the mole fraction of Dy in molten $(\mathrm{Dy}_{1/3},\mathrm{K})\mathrm{Cl}$ at 1093 K, Dy^{3+}: black circles, K^+: empty circles.

Table 3. Main experimental results and characteristic parameters obtained from the MD simulation at 1093 K.

x_{Dy}	κ_{exp} [24] (Sm^{-1})	κ_{cal} (Sm^{-1})	$b_{\mathrm{Dy,exp}}$ [13] ($10^{-8}\,\mathrm{m}^2\,\mathrm{V}^{-1}\,\mathrm{s}^{-1}$)	$b_{\mathrm{K,exp}}$ [13] ($10^{-8}\,\mathrm{m}^2\,\mathrm{V}^{-1}\,\mathrm{s}^{-1}$)	$\mathrm{SEV}_{\mathrm{Dy}}$ (ms^{-1})	$\mathrm{SEV}_{\mathrm{K}}$ (ms^{-1})	$D_{\mathrm{Dy,cal}}$ ($10^{-9}\,\mathrm{m}^2\,\mathrm{s}^{-1}$)	$D_{\mathrm{K,cal}}$ ($10^{-9}\,\mathrm{m}^2\,\mathrm{s}^{-1}$)
0	227	179.8	–	11.55	–	–	–	2.61
0.24	174	136.3	0.69±0.12	10.28±0.00	6.589	72.343	0.36	2.33
0.42	141	112.1	0.54±0.06	9.79±0.05	6.519	68.675	0.68	1.98
0.53	123	96.3	1.68±0.27	8.45±0.28	9.960	62.345	0.55	2.20
0.67	103	82.6	1.15±0.20	9.05±0.13	10.235	57.558	0.86	1.57
0.76	91.4	72.5	2.11±0.00	6.48±0.00	12.568	54.619	0.74	1.86
0.84	82.8	67.3	1.92±0.01	6.84±0.03	15.162	50.252	0.81	1.21
0.91	74.7	59.8	1.94±0.02	6.51±0.05	15.964	46.196	1.05	1.18
0.95	71.8	56.7	2.01±0.01	5.49±0.04	16.125	43.428	1.07	1.24
1.00	67.0	52.1	1.97	–	–	–	1.15	–

ies conjecture that there exist such species as $[\mathrm{LnCl}_6]^{3-}$ in the mixture system (KCl-LnCl_3) (Ln:La [24, 25], Y [26], Gd [27]). Neutron and X-ray diffraction studies of pure LnCl_3 melts also propose that even in the pure melts the octahedral unit exists, which is connected to other units by edge- or corner-sharing (LN:Y(neutron) [28], Nd(X-ray) [29], La, Ce, Pr, Nd, Gd, Dy and Sm (X-ray) [30]). X-ray diffraction has been performed also for a mixture melt of the composition $\mathrm{K}_3\mathrm{DyCl}_6$ [31]. The formation of such species as $[\mathrm{DyCl}_6]^{3-}$ with increasing x_{K} could be explained based on the coulombic interaction. Consequently, it seems that there is an approximately linear relation between two entities and the ionic behavior is reproduced by SEVs obtained from the simulation.

The self-diffusion coefficients of Dy and K for molten DyCl_3-KCl systems were calculated from the mean square displacements according to the Einstein expression [32]

$$D = \frac{1}{6}\frac{1}{d\tau}\langle\{r_i(t+\tau) - r_i(t)\}^2\rangle \tag{5}$$

as given in Fig. 5 and Table 3, which shows that the self-diffusion coefficient of Dy^{3+} increases with increasing concentration of Dy and the self-diffusion coefficient of K^+ increases with increasing the concentration of K. This is consistent with our calculated self-exchange velocities and the experimental internal cation mobilities. The tendency of the self-diffusion coefficient of Dy^{3+} and K^+ is consistent with the pair correlation functions, as expected.

On the other hand, the electric conductivity is calculated from the integral of the current autocorrelation function $j(t)$ according to Kubo's linear response theo-

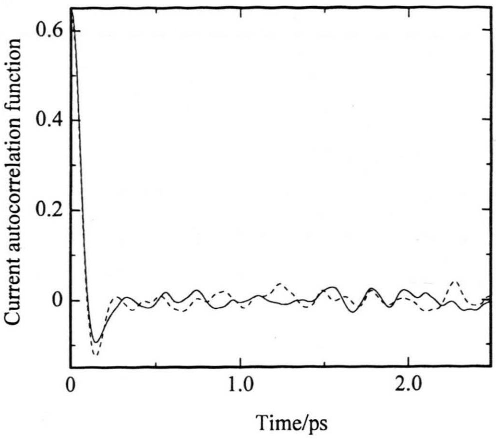

Fig. 6. Relationship between the current autocorrelation function and the time. $x_{Dy} = 0.24$: solid line, $x_{Dy} = 0.84$: broken line.

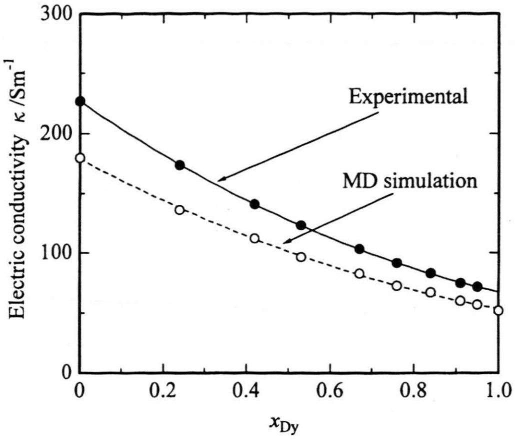

Fig. 7. Relationship between the electrical conductivity and the mole fraction of Dy. Experimental [24]: black circles and solid line, MD simulation: white circles and broken line.

ry [33], because the Nernst-Einstein equation could not be applied for molten salts conventionally:

$$\kappa = \frac{1}{kT} \int_0^\infty [j(0) \cdot j(t)], \tag{6}$$

where up to 10^7 MD steps are calculated. The current autocorrelation functions obtained from the MD simulations are shown in Figure 6. The first minimum of the autocorrelation function for the high concentration of $DyCl_3$ is deeper than that for the low concentration of $DyCl_3$, i.e., the electric conductivity at $x_{Dy} = 0.84$ is smaller than that at $x_{Dy} = 0.24$, as expected. The electric conductivity calculated from the MD simulation and measured is expressed in Figure 7. The tendency is reproduced by the MD simulation, i.e., the electric conductivity decreases with increasing concentration of Dy, although the values calculated from MD simulation are smaller than those measured [23].

4. Conclusion

This electromigration method could be used for effective separation of rare earth ions from alkali ions, because b_K and v_K are much (ca. 3–10 times) greater than b_{Dy} and v_{Dy} in the whole concentration range, as expected. As the concentration of Dy^{3+} increases, b_K, v_K, and D_K decrease considerably. This decrease is ascribed to the tranquilization effect by Dy^{3+} which strongly interacts with the Cl^- ions. As the concentration of K^+ increases, b_{Dy}, v_{Dy}, and D_{Dy} gradually decrease and become very small at high KCl concentrations. This decrease may be attributed to a promoted association of species containing Dy^{3+} and generation of the long-lived species $[DyCl_6]^{3-}$. In addition, we estimated the self-exchange velocity, self-diffusion coefficient and electrical conductivity in this system from the MD simulation. The orders of these parameters obtained from the MD simulation are consistent with the experimental results.

[1] M. Matsumiya and R. Takagi, Z. Naturforsch. To be submitted.
[2] M. Matsumiya, H. Matsuura, R. Takagi, and R. Fujita, J. Alloys Compd. **306,** 87 (2000).
[3] M. Matsumiya, R. Takagi, and R. Fujita, J. Nucl. Sci. Technol. **34,** 310 (1997).
[4] M. Matsumiya and R. Takagi, Z. Naturforsch. **55a,** 673 (2000).
[5] M. Matsumiya, M. Takano, R. Takagi, and R. Fujita, J. Nucl. Sci. Technol. **35,** 836 (1998).
[6] M. Matsumiya, M. Takano, R. Takagi, and R. Fujita, Z. Naturforsch. **54a,** 739 (1999).
[7] M. Matsumiya, R. Takagi, and R. Fujita, J. Nucl. Sci. Technol. **35,** 137 (1998).
[8] Y. I. Chang et al., ANL-IFR-246 (1994).
[9] M. Matsumiya and R. Takagi, Z. Naturforsch. **56a,** (2001) To be published.
[10] M. Matsumiya and R. Takagi, Z. Naturforsch. **55a,** 856 (2000).
[11] M. Matsumiya, H. Matsuura, R. Takagi, and Fujita, J. Electrochem. Soc. **147,** 11 (2000).
[12] M. Iwasaki and R. Takagi, J. Nucl. Sci. Technol. **31** [7], 751 (1994).
[13] R. Ohashi, M. Matsumiya, H. Matsuura, and R. Takagi, Electrochemistry **67,** 550 (1999).
[14] H. Matsuura, I. Okada, R. Takagi, and Y. Iwadate, Z. Naturforsch. **53a,** 45 (1998).
[15] M. P. Tosi and F. G. Fumi, J. Phys. Chem. Solids **25,** 45 (1964).
[16] J. E. Mayer, J. Chem. Phys. **1,** 270 (1933).

[17] M. Sakurai, R. Takagi, A. K. Adya, and M. Gaune-Escard, Z. Naturforsch. **53a,** 655 (1998).

[18] A. K. Adya, R. Takagi, Y. Sato, M. Gaune-Escard, A. C. Barnes and H. Fischer, to be submitted.

[19] B. Larsen, T. Forland, and K. Singer, Mol. Phys. **26,** 1521 (1973).

[20] P. P. Ewald, Ann. Phys. **64,** 253 (1921).

[21] L. V. Woodcock, Chem. Phys. Lett. **10,** 257 (1971).

[22] I. Okada, R. Takagi, and K. Kawamura, Z. Naturforsch. **35a,** 493 (1980).

[23] K. Fukushima, J. Mochinaga, T. Sekino, and Y. Iwadate, to be published.

[24] V. A. Maroni, E. J. Hathaway, and G. N. Papatheodorou, J. Phys. Chem. **78,** 1134 (1974).

[25] G. N. Papatheodorou, J. Chem. Phys. **66,** 2893 (1977).

[26] A. Matsuoka, K. Fukushima, K. Igarashi, Y. Iwadate, and J. Mochinaga, Nihon Kagaku Kaishi 471 (1993).

[27] M.-L. Saboungi, D. L. Price, C. Scamehorn, and M. P. Tosi, Europhys. Lett. **15,** 283 (1991).

[28] K. Igarashi, M. Kosaka, M. Ikeda, and J. Mochinaga, Z. Naturforsch. **45a,** 623 (1990).

[29] J. Mochinaga, Y. Iwadate, and K. Fukushima, Mater. Sci. Forum **73–75,** 147 (19991).

[30] Y. Iwadate, Y. Miyagi, M. Oowaki, K. Tanaka, and K. Fukushima, unpublished.

[31] N. Wax, Selected Papers on Noise and Stochastic Processes, Dover 1954.

[32] J. P. Hansen and I. R. McDonald, Theory of Simple Liquids, 2^{nd} ed., Academic Press, 1986.